AIAA SciTech Forum
6-10 January 2025, Orlando, FL
AIAA SCITECH 2025 Forum

10.2514/6.2025-2311

Numerical Study of NH_3/H_2-Air Ignition in Nanosecond Plasma Discharges with Non-Equilibrium Energy Transfer

Zhiyu Shi[1], Xingqian Mao[2]
Princeton University, Princeton, NJ 08544, USA

Ziyu Wang[3]
Utah State University, Logan, UT 84322, USA

Yiguang Ju[4]
Princeton University, Princeton, NJ 08544, USA

Ammonia (NH_3), with its higher energy density and easer storage and transportation as a hydrogen carrier, is emerging as a promising green alternative fuel. However, its application in power generation is limited by challenges such as a low burning velocity, slow oxidation at low temperatures, ignition difficulties, and nitrous oxide formation. This study computationally examines the role of non-equilibrium energy transfer with nanosecond discharges on NH_3 ignition and flame propagation in NH_3/H_2-air flows at 700 K and 1 atm using two-dimensional simulations. A non-monotonic relationship between ignition kernel volume and applied voltage is observed, with optimal ignition enhancement occurring at 200 Td. At this reduced electric field, the production of radicals and electronically excited species is maximized. The study identifies an optimal electrode gap size for a given pulse energy. While smaller gap sizes increase energy density, enhancing temperature and radical concentrations, overly small gaps restrict the ignition kernel size. A nonlinear dependency between pulse repetition frequency and ignition kernel volume is observed in nanosecond pulsed high-frequency discharges (NPHFD). There is an optimal frequency of plasma discharge for a given plasma energy and the number of discharge pulses. These findings provide valuable insights for designing controlled plasma discharge strategies to improve NH_3 ignition in reactive flows, with potential applications in internal combustion engines and gas turbines.

I. Introduction

The COP21 Paris Agreement [1] has catalyzed global efforts toward reducing carbon emissions and advancing sustainable energy solutions. Among the many alternative fuels explored, ammonia (NH_3) emerges as a promising candidate due to its renewable production potential and high hydrogen content [2-6]. With properties such as ease of liquefaction and carbon-neutral combustion, NH_3 offers an attractive alternative to hydrogen (H_2) for energy storage and transportation [2-3]. However, NH_3 still faces significant challenges to efficient combustion in engines and turbines [7-8], including a low burning velocity, elevated NO_x emissions, and poor low-temperature reactivity. Addressing these limitations requires enhancing NH_3's reactivity at low temperatures.

Advancements in plasma-assisted ignition technologies have revolutionized NH_3 combustion strategies [9-10]. Nanosecond plasma discharges, in particular, have demonstrated their capability to generate reactive species such as

---

[1] Ph.D. Candidate, Department of Mechanical and Aerospace Engineering.
[2] Postdoctoral Research Associate, Department of Mechanical and Aerospace Engineering.
[3] Assistant Professor, Department of Mechanical and Aerospace Engineering.
[4] Robert Porter Patterson Professor, Department of Mechanical and Aerospace Engineering, AIAA Fellow.

electrons, radicals, and ions, excited species, which can drastically lower ignition barriers [11-13]. These non-equilibrium processes enable novel pathways for NH_3 combustion at low temperatures. Experimental and numerical studies have explored the role of plasma discharges in enhancing NH_3 ignition [14-20]. Choe et al. [14] demonstrated that plasma-assisted flames could reduce NO_x emissions while improving flame stability under lean conditions. Zhong et al. [9] investigated plasma-assisted NH_3 oxidation at ambient conditions and developed a kinetic model incorporating non-equilibrium pathways. Mao et al. [15] computationally analyzed plasma-assisted NH_3/air ignition under nanosecond discharges, revealing that optimal ignition enhancement occurs at a reduced electric field of 250 Td, where radical production and electronic excitation are maximized. Similarly, Liu et al. [16] highlighted that H_2 blending influences NH_3 oxidation differently due to enhanced HO_2 formation and NO-driven pathways under plasma conditions. These studies have demonstrated the potential of non-equilibrium plasma in enhancing NH_3's reactivity at low temperatures.

However, current studies often rely on simplified models that fail to capture the intricate dynamics of plasma discharge and flame propagation in real-world applications, such as engines and turbines. Efficient NH_3 ignition and sustained combustion in these systems require a deeper understanding of the interactions between heat release, radical generation, and fluid dynamics. Mao et al. [21] examined the streamer propagation, its transition to spark and the ignition kernel development in H_2/air mixtures, highlighting the sensitivity of ignition enhancement to electrode geometry and electric field distribution. Lefkowitz and Ombrello [22-23] demonstrated the importance of the discharge interelectrode distance in forming effective ignition kernels in CH_4/air mixtures. More recently, nanosecond pulsed high-frequency discharges (NPHFD) have gained attention for their role in ignition enhancement [24-26]. Mao et al. [27] observed that for a fixed discharge energy, ignition kernel development in H_2/air flows is non-monotonically influenced by pulse frequency and number, indicating the need for optimized discharge parameters. Given NH_3's unique combustion characteristics, it is critical to explore its ignition and flame propagation under non-equilibrium plasma conditions using detailed chemistry and multi-dimensional modeling.

This study investigates the plasma-assisted ignition and flame propagation of NH_3/H_2-air mixtures under nanosecond discharges using two-dimensional (2D) simulations. The analysis addresses several key aspects: (1) the role of applied voltage and reduced electric field in electron energy deposition and ignition enhancement, (2) the influence of electrode gap size on ignition kernel development and flame propagation, and (3) the effects of discharge pulse frequency on radical accumulation and ignition efficiency for NPHFD. By identifying optimal non-equilibrium conditions, this work aims to advance ignition technologies for NH_3-based sustainable energy systems, contributing to the broader goal of energy innovation.

II. Numerical methods

The plasma modeling in this study is conducted using the 2D Multi-Scale Adaptive Reduced Chemistry Solver for Plasma-Assisted Combustion (MARCS-PAC), a tool developed at Princeton University [21, 27-29]. This framework integrates two solvers: the 2D plasma solver PASSKEy [30-32] and the adaptive reactive flow solver ASURF+ [33-36]. PASSKEy handles the drift-diffusion-reaction equations for plasma species, Helmholtz equations for photoionization, the Poisson equation for electric fields, and the energy conservation equation for plasma discharge. ASURF+ solves the unsteady, multi-component, reactive, compressible Navier-Stokes equations. These solvers are coupled using time-splitting methods, with detailed descriptions of the governing equations and numerical schemes provided in [21].

Simulations are performed for fuel-rich NH_3/H_2-air (0.190 NH_3/0.082 H_2/0.153 O_2/0.575 N_2) mixtures at an equivalence ratio of 1.2, 700 K, and 1 atm. Rich conditions are chosen to minimize NO_x emissions while increasing unburned NH_3, as typically done in gas turbines to balance NO_x mitigation with efficient oxidation. To initiate the discharge, a uniform pre-ionized mixture with an initial electron number density of $10^4\ \mathrm{cm}^{-3}$ is used [37], with initial ion densities ensuring quasi-neutrality. A nanosecond discharge with a single pulse is used to investigate the effects of applied voltage and electrode gap size, while nanosecond pulsed high-frequency discharges (NPHFD) are employed to study the influence of pulse repetition frequency. Each pulse features a trapezoidal voltage waveform with a peak of 1500–5000 V and a 2 ns rise time, with discharge duration adjusted to maintain constant plasma energy deposition across simulations.

The kinetic model for $NH_3/O_2/N_2$ mixtures, validated against experimental data [9], is employed. This comprehensive model includes 77 species and 894 reactions in the plasma kinetic sub-model, and 230 reactions in the combustion kinetic sub-model. The reaction rate constants with large uncertainties at low temperatures have been updated using experimental data as detailed in [9, 15]. To improve computational efficiency while maintaining accuracy, a reduced plasma model with 47 species and 71 reactions is developed. For combustion chemistry, the detailed $NH_3/H_2/O_2/N_2$ oxidation mechanism by Thorsen et al. [38] is employed, supplemented by an O_3 sub-model [39].

Figure 1 presents the 2D computational domain and axisymmetric geometry with needle-to-ring electrodes. To simplify 3D plasma modeling, the simulation domain is restricted to a 2D section, as indicated by the shaded region. The *R*-axis represents the radial direction of the electrode, while the *Z*-axis corresponds to the electrode's length and gas flow direction in cylindrical coordinates. The computational domain measures 3.5 mm by 15 mm, allowing sufficient space for undisturbed flow and flame propagation to observe ignition kernel evolution. Flow is introduced from the bottom at 20 m/s, maintaining the initial mixture composition, temperature, and pressure. Transparent boundary conditions are applied for other external boundaries, while reflective boundary conditions are used for the electrodes.

As shown in Fig. 1, the needle electrode is 4.3 mm long, with a 1 mm gap from the ring electrode unless otherwise specified. The ring electrode, positioned at Z = 2.7 mm, mitigates high electric fields near the sharp edges of the needle. The needle and ring radii are set to 60 μm and 40 μm, respectively, minimizing flow recirculation. To reduce computational costs, a fine, uniform mesh (10 × 10 μm) is used in the plasma discharge area, with a coarser mesh (40 × 40 μm) employed in outer regions.

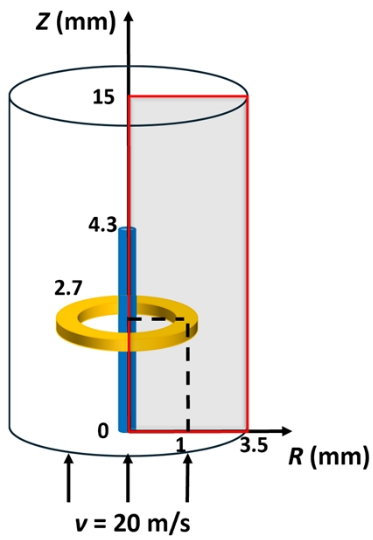

Fig. 1 2D computational domain and geometry.

III. Results and discussion

The effects of discharge voltage (U) on plasma-assisted ignition enhancement are analyzed, with a particular focus on how the reduced electric field E/N (the ratio of electric field strength to gas number density) influences non-equilibrium energy transfer. The applied peak pulse voltage varies between 1.5 kV and 5.0 kV, while the discharge energy is consistently maintained at 0.4 mJ. Figure 4(a) shows the time evolution of the ignition kernel volume for various applied voltages. Here, the ignition kernel volume is defined as the integrated region where the temperature exceeds 2000 K, which closely aligns with the flame front. In all cases, the ignition kernel volume increases over time. The most efficient ignition enhancement occurs at U = 2.0 kV, producing the largest ignition kernel volume at t = 0.3 ms. Figure 4 (b) shows the time evolution of the reduced electric field at the center of the discharge gap (R = 0.5 mm, Z = 2.75 mm). At U = 2.0 kV, the plateau after the initial breakdown corresponds to an E/N of approximately 200 Td, persisting until 10 ns. This suggests that $E/N \approx$ 200 Td is optimal for ignition enhancement.

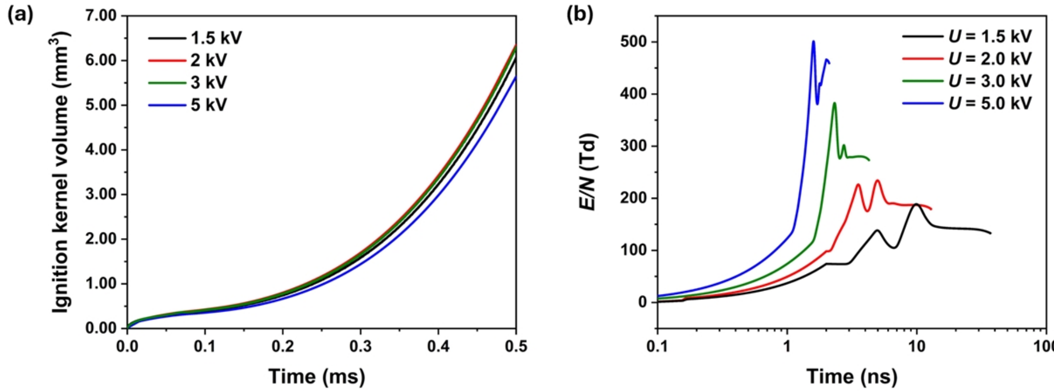

Fig. 2 Time evolution of (a) the ignition kernel volume and (b) the reduced electric field at the center of the discharge gap (R = 0.5 mm, Z = 2.75 mm) for different applied voltages, with a constant discharge energy of 0.4 mJ.

To explain the maximum ignition enhancement at U = 2.0 kV, Fig. 5(a) illustrates how electron energy is distributed among various modes as a function of E/N in the 0.190 NH_3/0.082 H_2/0.153 O_2/0.575 N_2 mixture, calculated using BOLSIG+ [40]. At E/N < 10 Td, most of the electron energy is directed toward rotational and vibrational excitation of NH_3. As E/N increases, energy deposition shifts primarily to N_2 vibrational excitation, with smaller contributions to the vibrational excitation of H_2 and O_2. With further increases in E/N, the rotational and vibrational excitation of NH_3 decreases, while energy deposition into NH_3 and O_2 dissociation, as well as N_2 electronic excitation, becomes more significant. In the range of 100 Td ≤ E/N ≤ 300 Td, the dominant pathways include the dissociation of NH_3, H_2, O_2, and N_2, along with the electronic excitation of N_2. At higher E/N values, ionization pathways are strongly enhanced. This could explain the non-equilibrium energy transfer and its role in ignition enhancement. An E/N of approximately 200 Td maximizes the production of electronically excited species and radicals, effectively reducing ignition delay time. This observation is consistent with the findings of [19].

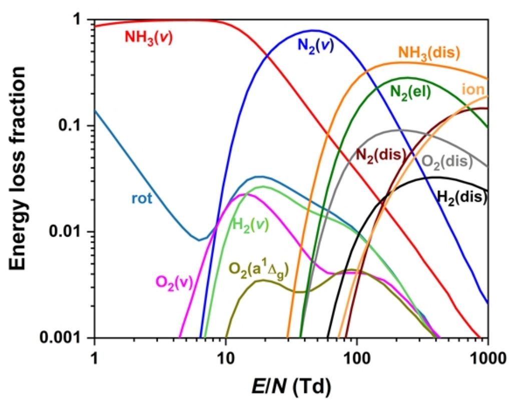

Fig. 3 Fractions of electron energy deposition into different excitation modes as a function of E/N in the 0.190 NH_3/0.082 H_2/0.153 O_2/0.575 N_2 mixture. (rot: rotational excitation; v: vibrational excitation; el: electronic excitation; dis: dissociation; ion: ionization)

Previous studies on plasma assisted H_2 ignition [21] have demonstrated that electrode gap size significantly impacts the spatial distribution of discharge energy. To investigate this effect in plasma-assisted NH_3/H_2-air ignition, simulations are conducted with electrode gap sizes (D) ranging from 0.35 mm to 0.8 mm, while maintaining a constant applied voltage of 5.0 kV and discharge energy of 0.2 mJ. Figure 4 (a) illustrates the time evolution of ignition kernel volume for different gap sizes. The results reveal a non-monotonic relationship between ignition kernel volume and electrode gap size, with the most effective ignition enhancement observed at D = 0.50 mm. Excessively large gap sizes can lead to ignition failure due to the increased critical ignition radius. Fig. 4(b) presents the distributions of temperature at t = 150 ns and Z = 2.75 mm. This distribution pattern demonstrates that smaller electrode gap sizes increase the energy density and thus elevate temperatures within the discharge region. With an effective ignition threshold defined at 2000 K, optimal ignition is achieved at D = 0.50 mm, where the temperature throughout the discharge region consistently exceeds this threshold, maximizing the ignition kernel area. In contrast, for $D = 0.80$ mm, ignition is limited to a small region near the needle electrode. At $D = 0.35$ mm, the highest reduced electric field and concentrated energy deposition result in the highest temperature. However, the narrower discharge region restricts the ignition kernel area compared to $D = 0.50$ mm.

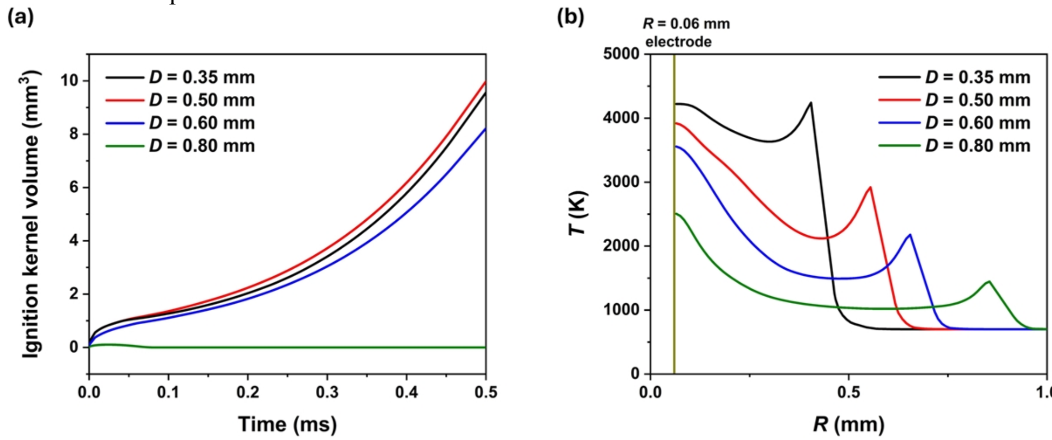

Fig. 4 (a) Time evolutions of the ignition kernel volume across different electrode gap sizes at the same discharge energy of 0.2 mJ. (b) Distributions of temperature along the *R*-axis direction at $t = 150$ ns and $Z = 2.75$ mm across different electrode gap sizes. The dark yellow line indicates the needle electrode.

To investigate the synergistic effects of multiple discharge pulses on ignition, two consecutive pulses with identical discharge energy but varying pulse repetition frequencies (f) are analyzed. The pulse energy of each pulse is 0.2 mJ, with an applied voltage of 5.0 kV and an electrode gap size of 1.0 mm. It is noted that a single pulse of 0.2 mJ is insufficient to ignite the mixture. Figure 12 illustrates the ignition kernel volume at different pulse repetition frequencies, with dashed lines representing the ignition kernel volume for a single 0.4 mJ pulse. To further analyze the ignition kernel development, two specific time points, $t = 0.3$ ms and $t = 0.5$ ms, are considered. At lower pulse repetition frequencies, ignition enhancement is less effective than with a single pulse, primarily due to radical quenching and heat loss during the interval between pulses. However, when the pulse repetition frequency exceeds 100 kHz, ignition is significantly enhanced. The optimal frequency is determined to be 500 kHz, where the ignition kernel volume increases by 98.7% at $t = 0.3$ ms and 68.4% at $t = 0.5$ ms compared to the single-pulse case. Beyond this frequency, further increases lead to a decline in ignition kernel volume. As the pulse repetition frequency approaches infinity, the two pulses effectively merge, producing ignition behavior similar to that of a single pulse with 0.4 mJ energy.

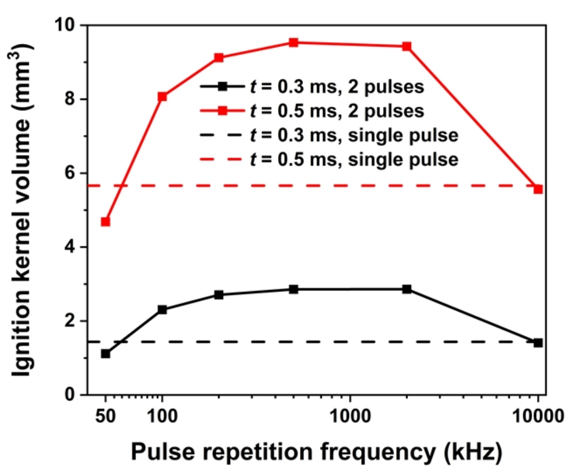

Fig. 5 Ignition kernel volume with different pulse repetition frequencies at $t = 0.3$ and 0.5 ms. In the cases with 2 pulses, the discharge energy per pulse is set to 0.2 mJ. The dashed lines mark the ignition kernel volume for a single pulse of 0.4 mJ.

IV. Conclusion and future work

This study computationally examines the effects of non-equilibrium energy transfer, plasma properties, and electrode gap size on NH_3 ignition and flame propagation using nanosecond discharges. The findings reveal a non-monotonic relationship between ignition energy, and ignition kernel volume as well as the applied plasma voltage, frequency, and the number pulses. It is shown that an *E/N* value of approximately 200 Td provides the highest ignition enhancement due to enhanced radical production via electron impact reactions and contributions from electronically excited species. Moreover, a non-monotonic dependency is observed between the ignition kernel volume and electrode gap size, with the optimal enhancement occurring at a gap size of 0.5 mm. The results show that larger gap sizes result in ignition failure due to lower energy density combined with heat loss and quenching effects. On the other hand, smaller gap sizes limit the ignition kernel size, preventing it from exceeding the critical ignition radius. Lastly, the study shows that with a fixed total discharge energy, the pulse repetition frequency significantly influences ignition enhancement in nanosecond pulsed high-frequency discharges. The optimal pulse repetition frequency is found to be 500 kHz. This is due to the overlap of the second pulse with the existing ignition kernel, which increases the reduced electric field, accelerates radical accumulation, and enlarges the ignition kernel. These findings will provide insights on developing controlled plasma discharge techniques to achieve efficient NH_3 ignition in reactive flows within internal combustion engines and gas turbines.

Acknowledgements

This work is supported by the DOE grant DE-SC0020233 of Plasma Science Center and the PPPL Plasma Science and Technology fellowship.

References

[1] United Nations, The Paris Agreement, 2015, available at http://unfccc.int/files/essential_background/convention/application/pdf/english_paris_agreement.pdf.
[2] A. Valera-Medina, H. Xiao, M. Owen-Jones, W.I. David, P. Bowen, Ammonia for power, *Progress in Energy and combustion science* 69 (2018) 63-102.
[3] H. Kobayashi, A. Hayakawa, K.K.A. Somarathne, E.C. Okafor, Science and technology of ammonia combustion, *Proceedings of the Combustion Institute* 37 (2019) 109-133.
[4] F. Chang, W. Gao, J. Guo, P. Chen, Emerging materials and methods toward ammonia‐based energy storage and conversion, *Adv. Mater.* 33 (2021) 2005721.
[5] J. Lim, C.A. Fernández, S.W. Lee, M.C. Hatzell, Ammonia and nitric acid demands for fertilizer use in 2050, *ACS Energy Lett.* 6 (2021) 3676-3685.
[6] F. Guo, C. Li, X. Xiu, K. Cheng, J. Qin, Comprehensive technical analyses of a solid oxide fuel cell turbine-less hybrid aircraft propulsion system using ammonia and methane as alternative fuels, *Appl. Therm. Eng.* 230 (2023) 120787.
[7] C. Lhuillier, P. Brequigny, F. Contino, C. Mounaïm Rousselle, Experimental study on ammonia/hydrogen/air combustion in spark ignition engine conditions, *Fuel* 269 (2020) 117448.
[8] S.W. Kim, A. Heckel, S. McKeen, G. Frost, E.Y. Hsie, M. Trainer, A. Richter, J. Burrows, S. Peckham, G. Grell, Satellite‐observed US power plant NOx emission reductions and their impact on air quality, *Geophys. Res. Lett.* 33 (2006).
[9] H. Zhong, X. Mao, N. Liu, Z. Wang, T. Ombrello, Y. Ju, Understanding non-equilibrium N_2O/NO_x chemistry in plasma-assisted low-temperature NH_3 oxidation, *Combustion and Flame* 256 (2023) 112948.
[10] A. Bogaerts, E.C. Neyts, Plasma technology: an emerging technology for energy storage, *ACS Energy Lett.* 3 (2018) 1013-1027.
[11] Y. Ju, W. Sun, Plasma assisted combustion: Dynamics and chemistry, *Progress in Energy and Combustion Science* 48 (2015) 21-83.
[12] Y. Ju, J.K. Lefkowitz, C.B. Reuter, S.H. Won, X. Yang, S. Yang, W. Sun, Z. Jiang, Q. Chen, Plasma assisted low temperature combustion, *Plasma Chemistry and Plasma Processing* 36 (2016) 85-105.
[13] A. Starikovskiy, N. Aleksandrov, Plasma-assisted ignition and combustion, *Progress in Energy and Combustion Science* 39 (2013) 61-110.
[14] J. Choe, W. Sun, T. Ombrello, C. Carter, Plasma assisted ammonia combustion: Simultaneous NO_x reduction and flame enhancement, *Combustion and Flame* 228 (2021) 430-432.
[15] X. Mao, H. Zhong, N. Liu, Z. Wang, Y. Ju, Ignition enhancement and NO_x formation of NH_3/air mixtures by non- equilibrium plasma discharge, *Combustion and Flame* 259 (2024) 113140.
[16] N. Liu, B. Mei, X. Mao, Z. Wang, Z. Sun, Y. Xu, Z. Shi, Y. Ju, Kinetics of low temperature plasma assisted NH_3/H_2 oxidation in a nanosecond-pulsed discharge, *Proceedings of the Combustion Institute* 40 (2024) 105353.
[17] Choe, Jinhoon, and Wenting Sun. "Experimental investigation of non-equilibrium plasma-assisted ammonia flames using NH2* chemiluminescence and OH planar laser-induced fluorescence." *Proceedings of the Combustion Institute* 39.4 (2023): 5439-5446.

[18] Taneja, Taaresh Sanjeev, Praise Noah Johnson, and Suo Yang. "Nanosecond pulsed plasma assisted combustion of ammonia-air mixtures: Effects on ignition delays and NO_x emission." *Combustion and Flame* 245 (2022): 112327.
[19] Mao, Xingqian, Hongtao Zhong, Ning Liu, and Yiguang Ju. "Ignition enhancement of NH3/air mixtures by non-equilibrium excitation in a nanosecond pulsed plasma discharge." *AIAA SCITECH 2023 Forum*, p. 0748. 2023.
[20] Zhong, Hongtao, Ning Liu, Xingqian Mao, Ziyu Wang, and Yiguang Ju. "Kinetic studies of low-temperature ammonia oxidation in a nanosecond repetitively-pulsed discharge." *AIAA SCITECH 2023 Forum*, p. 1694. 2023.
[21] Mao, Xingqian, et al. "Modeling of the effects of non-equilibrium excitation and electrode geometry on H_2/air ignition in a nanosecond plasma discharge." *Combustion and Flame* 240 (2022): 112046.
[22] J.K. Lefkowitz, T. Ombrello, An exploration of inter-pulse coupling in nanosecond pulsed high frequency discharge ignition, *Combustion and Flame* 180 (2017) 136–147.
[23] J.K. Lefkowitz, T. Ombrello, Reduction of flame development time in nanosecond pulsed high frequency discharge ignition of flowing mixtures, *Combustion and Flame* 193 (2018) 471–480.
[24] Lefkowitz, Joseph K., et al. "Elevated OH production from NPHFD and its effect on ignition." *Proceedings of the Combustion Institute* 38.4 (2021): 6671-6678.
[25] Opacich, Katherine C., et al. "Analyzing the ignition differences between conventional spark discharges and nanosecond-pulsed high-frequency discharges." *Proceedings of the Combustion Institute* 38.4 (2021): 6615-6622.
[26] Lefkowitz, Joseph K., and Timothy Ombrello. "An exploration of inter-pulse coupling in nanosecond pulsed high frequency discharge ignition." *Combustion and Flame* 180 (2017): 136-147.
[27] Mao, Xingqian, et al. "Effects of inter-pulse coupling on nanosecond pulsed high frequency discharge ignition in a flowing mixture." *Proceedings of the Combustion Institute* 39.4 (2023): 5457-5464.
[28] T.Y. Chen, X. Mao, H. Zhong, Y. Lin, N. Liu, B.M. Goldberg, Y. Ju, and E. Kolemen. Impact of CH_4 addition on the electron properties and electric field dynamics in a Ar nanosecond-pulsed dielectric barrier discharge. *Plasma sources science and technology* 31.12 (2023) 125013.
[29] M. Vorenkamp, S. Steinmetz, X. Mao, Z. Shi, A. Starikovskiy, Y. Ju, and C. Kliewer. Effect of plasma-enhanced low-temperature chemistry on deflagration-to-detonation transition in a microchannel. *AIAA J.* 61.11 (2023) 4821-4827.
[30] Y. Zhu, X. Chen, Y. Wu, S. Starikovskaia. PASSKEy code [software]. Available from http://www.plasma-tech.net/parser/passkey/(Science and Technology of Plasma Dynamics Laboratory, Xi'an, China and Laboratoire de Physique des Plasmas, Paris, France, 2021).
[31] Y. Zhu, S. Shcherbanev, B. Baron, S. Starikovskaia, Nanosecond surface dielectric barrier discharge in atmospheric pressure air: I. Measurements and 2D modeling of morphology, propagation and hydrodynamic perturbations, *Plasma sources science and technology* 26 (2017) 125004.
[32] Y. Zhu, X. Chen, Y. Wu, J. Hao, X. Ma, P. Lu, P. Tardiveau, Simulation of the ionization wave discharges: a direct comparison between the fluid model and E–FISH measurements, *Plasma Sources Sci. Technol.* 30 (2021) 075025.
[33] Z. Chen, M. Burke, Y. Ju, Effects of Lewis number and ignition energy on the determination of laminar flame speed using propagating spherical flames, *Proceedings of the Combustion Institute* 32 (2009) 1253-1260.
[34] Z. Chen, Studies on the Initiation, Propagation, and Extinction of Premixed Flames, The Department of Mechanical and Aerospace Engineering, Princeton University, Princeton, NJ, 2009.
[35] W. Sun, Developments of Efficient Numerical Methods for Combustion Modeling with Detailed Chemical Kinetics, The Department of Mechanical and Aerospace Engineering, Princeton University, Princeton, NJ, 2020.
[36] T. Zhang, W. Sun, L. Wang, Y. Ju, Effects of low-temperature chemistry and turbulent transport on knocking formation for stratified dimethyl ether/air mixtures, *Combustion and Flame* 200 (2019) 342–353.
[37] S. Pancheshnyi, Role of electronegative gas admixtures in streamer start, propagation and branching phenomena, *Plasma Sources Science and Technology* 14.4 (2005): 645.
[38] L.S. Thorsen, M.S. Jensen, M.S. Pullich, J.M. Christensen, H. Hashemi, P. Glarborg, V.A. Alekseev, E.J. Nilsson, Z. Wang, B. Mei, High pressure oxidation of NH_3/n-heptane mixtures, *Combustion and Flame* 254 (2023) 112785.
[39] H. Zhao, X. Yang, Y. Ju, Kinetic studies of ozone assisted low temperature oxidation of dimethyl ether in a flow reactor using molecular-beam mass spectrometry, *Combustion and Flame* 173 (2016) 187-194.
[40] G. Hagelaar, L.C. Pitchford, Solving the Boltzmann equation to obtain electron transport coefficients and rate coefficients for fluid models, *Plasma sources science and technology* 14 (2005) 722.